11th World Congress on Computational Mechanics (WCCM XI)
5th European Conference on Computational Mechanics (ECCM V)
6th European Conference on Computational Fluid Dynamics (ECFD VI)
E. Oñate, J. Oliver and A. Huerta (Eds)

VORTEX ELEMENT METHOD SCHEME FOR NUMERICAL SIMULATION IN FSI-PROBLEM FOR CLAMPED-CLAMPED CYLINDRICAL SHELL

ANDREY V. ERMAKOV*, ILIA K. MARCHEVSKY† AND GEORGY A. SHCHEGLOV*

* Aerospace Systems department,
Bauman Moscow State Technical University,
2nd Baumanskaya st., 5, 105005 Moscow, Russia
e-mail: georg@energomen.ru

† Applied Mathematics department
Bauman Moscow State Technical University,
2nd Baumanskaya st., 5, 105005 Moscow, Russia
e-mail: iliamarchevsky@mail.ru

Key words: Vortex Element Method, Incompressible Medium, Vorticity, Vorton, Aeroelasticity, Elastic Cylindrical Shell, Frequency Spectrum, Flow Induced Vibrations

Abstract. Pure lagrangian vortex methods are suitable for engineering analysis when it is necessary to compute unsteady aerodynamic loads in complicated FSI-problems. Lagrangian vortex element methods allow to simulate dynamics of 3D vortex structures with small numerical diffusion because in these methods vorticity is 'primitive' variable and integral formulation of governing equations is used. Computational cost of these methods is small in comparison with grid CFD methods. In the present research the vortex element method with vortex fragmentons is used for clamped-clamped elastic cylindrical shell oscillations simulation exited by unsteady hydrodynamic loads. Shell dynamics is simulated using modal analysis method; normal modes are calculated using MSC.Nastran software.

1 INTRODUCTION

Cylindrical structure elements interacting with the flow are widespread in different engineering systems. In case of rigid circular cylinder hydrodynamic loads are unsteady but close to monoharmonic with dimensionless frequency St $\approx$ 0.2, so the simplified mathematical models are often used in technical applications. But if thin elastic shell is considered and it is necessary to simulate its dynamics in the flow, the influence is hydroelastic vibrations should be taken into account. This problem — ovalling oscillations

investigation for cylindrical shells in cross flow is well-known [1]. Hydrodynamic loads in this case are poly-harmonic, and this phenomenon can be important in structural analysis.

The numerical simulation of the shell dynamics in such coupled FSI-problem is complicated since it requires computation of unsteady hydrodynamic loads induced by detached flow around the deformable shell. As it is shown in [5] for 2D-case, unsteady intensive vortex shedding significantly influences hydrodynamic loads for elastic airfoils. For 3D case such influence also is supposed to be even more significant.

Widespread grid methods can be used for 3D FSI-problems solving but they require too many computational resources, mainly time of computations, memory and disk space. In case of structure optimization process when it is necessary to investigate number of alternatives, this restriction becomes weighty. So in engineering analysis the other class of CFD methods — Lagrangian vortex methods can be more suitable.

Vortex element methods are well-known and well-developed for vortex structures dynamics simulation in unbounded regions because perturbation-decay boundary condition is satisfied automatically. However boundary condition on body surface satisfaction is non-trivial problem. There are approaches based on Discrete Vortices Method [2], Vorticity Flux approach [3], some other ideas [6]. Vorticity flux-based approach shows its advantages when solving coupled FSI-problems with deformable bluff bodies.

In this research the original numerical algorithm based on vortex element method is developed for coupled 3D problem of shell-flow interaction. This algorithm is verified on experimental data [7] for clamped-clamped elastic shell oscillations.

2 GOVERNING EQUATIONS

The cylindrical shell with radius R, length L and wall thickness h is considered in unbounded incompressible flow with constant incoming flow velocity $\mathbf{V}_\infty$. The shell is supposed to be closed and clamped at cutting faces, so only external flow is considered (fig. 1).

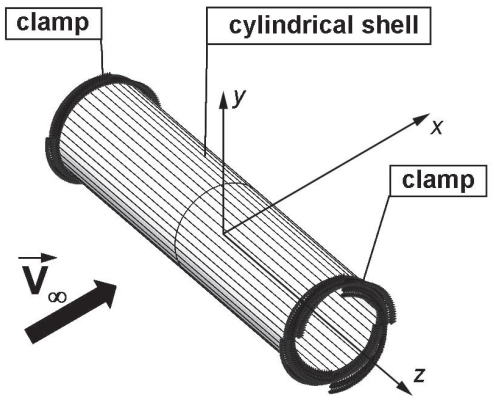

Figure 1: Cylindrical shell in the cross flow

Shell material with density γ is assumed to be deformable with modulus of elasticity E and Poisson ratio ν. Flow viscosity is sufficiently small so it is possible to take it into account only as a cause of vortex shedding on shell surface. The flow far from the shell is assumed to be inviscid.

Mathematical model of this FSI-problem consists of 2 groups of equations and corresponding boundary and initial conditions. Shell dynamics is described by the following equations:

$$B\left(\frac{\partial^2}{\partial\alpha^2}+\frac{1-\nu}{2}\frac{\partial^2}{\partial\beta^2}\right)u+B\frac{1+\nu}{2}\frac{\partial^2 v}{\partial\alpha\partial\beta}+B\frac{\nu}{R}\frac{\partial\omega}{\partial\alpha}=\gamma h\frac{\partial^2 u}{\partial t^2},$$

$$B\frac{1+\nu}{2}\frac{\partial^2 u}{\partial\alpha\partial\beta}+B\left(\frac{1-\nu}{2}\frac{\partial^2}{\partial\alpha^2}+\frac{\partial^2}{\partial\beta^2}\right)v+\frac{B}{R}\frac{\partial\omega}{\partial\beta}=\gamma h\frac{\partial^2 v}{\partial t^2},$$

$$B\frac{\nu}{R}\frac{\partial u}{\partial\alpha}+\frac{B}{R}\frac{\partial v}{\partial\beta}+\left(\frac{B}{R^2}+D\nabla^2\nabla^2\right)\omega+\gamma h\frac{\partial^2\omega}{\partial t^2}=Q_H(p(\mathbf{r}_K,t)),$$

$$u|_{t=0}=0,\quad v|_{t=0}=0,\quad w|_{t=0}=0,$$

$$\left.\frac{\partial u}{\partial t}\right|_{t=0}=0,\quad \left.\frac{\partial v}{\partial t}\right|_{t=0}=0,\quad \left.\frac{\partial w}{\partial t}\right|_{t=0}=0,$$

$$u|_{\alpha=0,L}=v|_{\alpha=0,L}=w|_{\alpha=0,L}=\left.\frac{\partial w}{\partial\alpha}\right|_{\alpha=0,L}=0.$$

Here $B=Eh/(1-\nu^2)$ and $D=Eh^3/(12(1-\nu^2))$ are shell elastic characteristics; α and β are coordinates on the middle surface of the shell in lengthwise direction and circumferential direction respectively; u, v and w are shell displacements which determine positions of points $\mathbf{r}_K$ on the deformed shape; ∇ is Hamilton differential operator. Hydrodynamic loads Q_H are assumed to be normal to the surface (i.e., only pressure p is taken into account), shear stress is neglected because of small flow viscosity.

Incompressible fluid dynamics is described by Navier — Stokes equations:

$$\nabla\cdot\mathbf{V}=0,$$

$$\frac{\partial\mathbf{V}}{\partial t}+(\mathbf{V}\cdot\nabla)\,\mathbf{V}=\frac{\mu}{\rho}\nabla^2\mathbf{V}-\nabla\left(\frac{p}{\rho}\right),$$

$$\mathbf{V}(\mathbf{r},t_0)=\mathbf{V}_0,\quad \lim_{r\to\infty}\mathbf{V}=\mathbf{V}_\infty,\quad \lim_{r\to\infty}p=p_\infty,$$

$$\mathbf{V}(\mathbf{r}_K,t)=\dot{\mathbf{r}}_K.$$

Here $\mathbf{V}$ is flow velocity; p is pressure; $\rho=\text{const}$ is flow density; μ is viscosity coefficient, $\mathbf{r}_K$ is position of point on the deformed shape, $\mathbf{r}_K=\mathbf{r}_{0K}+\mathbf{u}(u,v,w,t)$; $\mathbf{r}_{0K}$ is position of the corresponding point at initial time on cylindrical surface.

So the coupling of both subsystems is provided by moving boundary $\mathbf{r}_K$ of the shell. Its displacement is determined by fluid pressure. At the same time pressure distribution depends on vorticity evolution near moving wall.

3 NUMERICAL METHOD

An original numerical algorithm is developed for above mentioned governing equations solving. Meshless lagrangian vortex element method is used for flow simulation. The vortex fragmenton model [8] is used as common vortex element for both vortex wake and vortex layer on the surface representation. In order to satisfy no-slip boundary condition on the body closed surface vortex frameworks are constructed on the panels which approximate the surface (fig. 2). Panels' vertexes displacements can be set by generalized vector $\{q\}$ which describes displacements u, v and w of the elastic shell. There is collocation point $\mathbf{k}_0^j$ placed in the center of j^{th} panel and normal unit vector $\mathbf{n}_0^j$. Every vortex framework is placed on small distance β from the corresponding panel and consists of m_j vortex fragmentons which are characterized by marker positions $\mathbf{r}_s^j$ and fragmenton vectors $\mathbf{h}_s^j$, $s = 1, \ldots, m_j$.

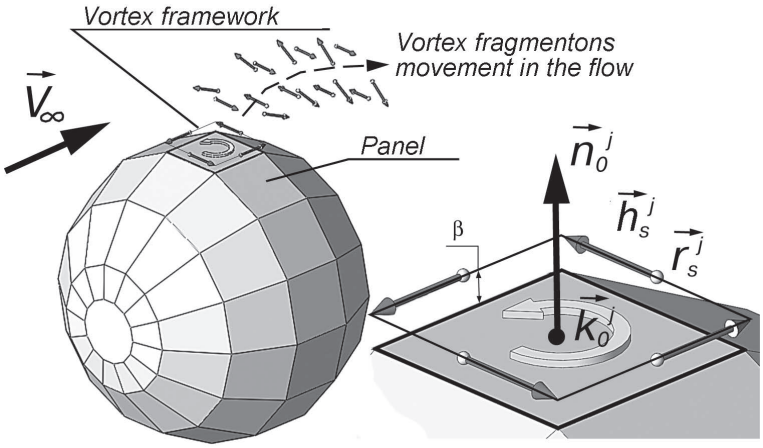

Figure 2: Vortex framework on the panel on body surface

Vortex frameworks circulation can be computed from the equivalence condition for normal velocities of the flow and the surface which is the same as in Discrete Vortex Method [2]. Then according to vorticity flux model developed by Lighthill & Chorin [3, 9] all the vorticity from surface vortex layer becomes free and moves in the flow. In order to simulate such vorticity flux vortex frameworks are split up into separate vortex fragmentons (fig. 2).

It should be noted that there exists another approach to vortex layer intensity on the surface computation. It is based on the equivalence of tangent velocities of the surface and flow and also leads to integral equation [10].

In order to compute pressure distribution $p(\mathbf{r}, t)$ in the flow the analog of the Bernoulli and Cauchy-Lagrange integrals is used [11]. For numerical solution of vortex fragmenton dynamics equations explicit Euler method is used [8] with fixed time step Δt.

Shell dynamics partial differential equations can be transformed at every time step to linear ordinary differential equations for panels' vertexes displacement vector $\{q\}$ components:

$$[M]\{\ddot{q}\} + [K]\{\dot{q}\} + [C]\{q\} = \{F_H\}. \tag{1}$$

Here $[M]$, $[K]$ and $[C]$ are mass, damping and stiffness matrices; $\{F_H\}$ is reduced hydrodynamic forces vector.

It is important that $\{F_H\}$ vector assumed to be constant during time step. It allows to use normal mode transient analysis method for computing vertexes' displacements $\{q(t_{n+1})\}$ at the next time step for given 'initial' displacements $\{q(t_n)\}$. At initial time moment $\{q(t_0)\} = \{0\}$.

Denoting normal modes generalized coordinates as $\{\phi\}$ and eigenforms matrix as $[A]$, equation (1) can be written down in the following form:

$$\{\ddot{\phi}\} + \delta[\omega]_{\text{diag}}\{\dot{\phi}\} + [\omega^2]_{\text{diag}}\{\phi\} = \{f_H\}, \quad \{q\} = [A]\{\phi\}. \tag{2}$$

Here δ is constant damping coefficient (modal damping decrements are assumed to be proportional to eigenfrequencies); $[\omega]_{\text{diag}}$ is diagonal matrix consist of lower eigenfrequencies, $[\omega^2]_{\text{diag}} = [\omega]_{\text{diag}} \cdot [\omega]_{\text{diag}}$; $\{f_H\}$ is generalized hydrodynamic forces vector, $\{f_H\} = [A]^T\{F_H\}$.

Eigenfrequencies and eigenforms matrices $[\omega]_{\text{diag}}$ and $[A]$ are computed using Finite Element Method software MSC.Nastran with SOL103 solver. Surface mesh on the shell is built with Patran preprocessor, and it is used both for dynamics analysis and flow simulation. Nodes of QUAD4 shell elements are the same as the panels vertexes. Algorithm scheme of FEM analysis and mesh constructing is shown on fig. 3.

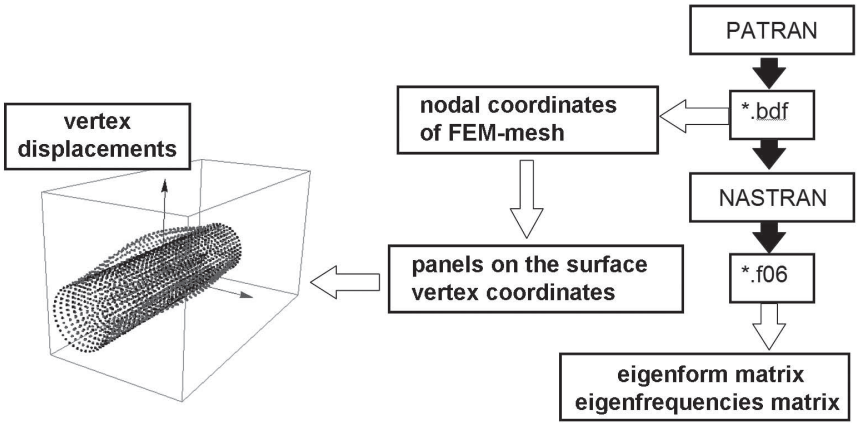

Figure 3: Scheme of FEM analysis and mesh constructing using MSC.Nastran and Patran

So the developed numerical algorithm consists of two subsystems: elastic subsystem and hydrodynamic one. These subsystems are coupled via vortex layer intensity computation procedure.

At every time step t_n firstly no-slip boundary condition are satisfied in panels' collocation points $\mathbf{k}_0^j$, then new vortex fragmentons are generated from the corresponding vortex frameworks and finally pressure distribution and $\{F_H\}$ vector for system (1) are computed. Vortex fragmentons displacements are computed according to the algorithm described in [8]. Since system (2) consists of independent ordinary linear differential equations with constant coefficients, it can be solved analytically:

$$\phi_k(t_{n+1}) = \frac{f_{Hk}}{\omega_k^2} + \frac{\exp(-\delta\omega_k\Delta t)}{\Omega_k\omega_k} \times \\ \times \left\{ [\Omega_k\omega_k\phi_k(t_n) - f_{Hk}]\cos(\Omega_k\Delta t) + \left[\omega_k\dot{\phi}_k(t_n) + \delta\left(\omega_k^2\phi_k(t_n) - f_{Hk}\right)\right]\sin(\Omega_k\Delta t)\right\}$$

$$\dot{\phi}_k(t_{n+1}) = \frac{\omega_k\exp(-\delta\omega_k\Delta t)}{\Omega_k} \times \\ \times \left\{ \left[\frac{\Omega_k}{\omega_k}\phi_k(t_n)\right]\cos(\Omega_k\Delta t) + \left[\frac{f_k}{\omega_k} - \left(\delta\dot{\phi}_k(t_n) + \omega_k\phi_k(t_n)\right)\right]\sin(\Omega_k\Delta t)\right\},$$

where $\Omega_k = \omega_k\sqrt{1-\delta^2}$, index k denotes number of eigenform.

The obtained results allow to compute vertex displacements vector $\{q\}$ and construct the deformed shape of the body surface at the next time step t_{n+1}.

4 NUMERICAL EXPERIMENT

The main aim of the numerical experiment was verification of the developed algorithm with respect to known experimental data [12]. In this experiment thin shell with dimensions $R = 0.0578$ m, $L = 0.512$ m, $h = 0.0003$ m made from steel ($E = 1.98 \cdot 10^{11}$ Pa, $\nu = 0.31$, $\gamma = 7920$ kg/m^3) was placed on moving trolley in water ($\rho = 1000$ kg/m^3). Damping coefficient was $\delta = 0.05$.

CAE-model of the shell consisting of 1400 panels was constructed in Patran (40 panels in circumferential direction, 32 panels in lengthwise direction, 120 panels on tips).

For flow simulation using vortex element method vortex fragmenton smoothing radius $\varepsilon = 0.004$ m was chosen, distance from the panel to vortex framework was $\beta = 0.004$ m.

Two values of incoming flow velocity were considered: $V_\infty = 0.9$ m/s and $V_\infty = 4.0$ m/s which correspond to subcritical and supercritical flows. Time steps were chosen equal to $\Delta t = 0.008$ s and $\Delta t = 0.001$ s respectively.

Pressure distribution in [12] was calculated on the basis of empirical formulae [13] obtained for rigid cylinder. So the first verification test included pressure distribution comparison between vortex element method simulation for rigid cylinder and [13].

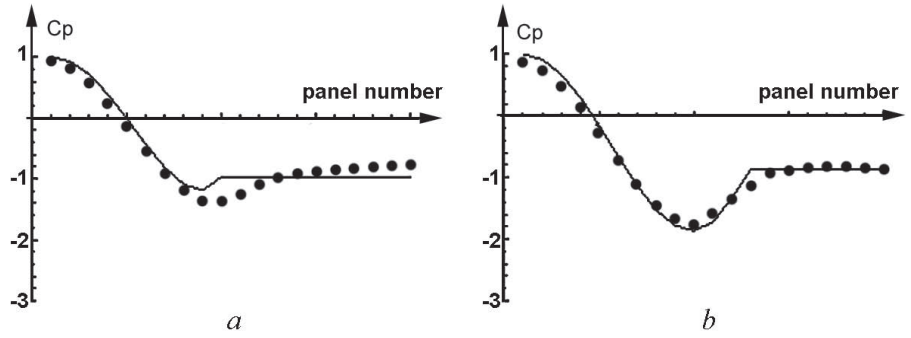

Figure 4: Pressure coefficient C_p distribution around the middle ($z = 0$) cross-section of the rigid cylinder for subcritical (a) and supercritical (b) flows. Dots (•) correspond to numerical simulation results, averaged over 800 time steps; line (—) corresponds to empirical formulae [13]

The obtained results are shown on fig. 4; results of numerical simulation are close to experimental data.

Vortex shedding frequency in the numerical experiment was about 1.32 Hz which corresponds to Strouhal number $\mathrm{St}_* = 0.17$.

As the second test the transient states were simulated for elastic shell interacting with cross-flow. The lowest shell eigenfrequency computed using MSC.Nastran was $\omega_1 = 399.3$ Hz. In modal analysis 48 eigenforms were used; it was a minimal number which provided correct results of simulation. The highest eigenfrequency was $\omega_{48} = 1550.4$ Hz.

In numerical simulation two cases have been considered. In the first one static problem was investigated in MSC.Nastran for the clamped-clamped shell with given pressure distribution [13], in the second one unsteady simulation using the developed algorithm was carried out. The results are shown on fig. 5. The averaged displacements in the middle cross-section obtained in numerical simulation are in good agreement with static displacements and experimental data. As an example, the 3D deformed shape of the elastic shell at some time moment is shown on fig. 6. Vortex wake around the cylinder is shown on fig. 7.

Unsteady drag and lift dimensionless coefficients analysis allows to draw the following conclusion. Drag coefficient $C_x \approx 0.9$ is almost constant both for rigid and elastic shells. In their spectrums there are no peaks with the exception of doubled Strouhal number $2\mathrm{St}_* \approx 0.34$, time dependencies for $C_x(t)$ are almost monoharmonic for rigid and elastic shells.

The main difference between rigid and elastic shells is in lift coefficients C_y spectrum (fig. 8). As it shown, $C_y(t)$ time dependency for rigid cylinder is almost monoharmonic ($\mathrm{St}_* = 0.17$), but for elastic shell it becomes polyharmonic; its main modes correspond to Strouhal numbers $\mathrm{St}^{(1)} = 0.06$, $\mathrm{St}^{(2)} = 0.20$. These results are in good agreement with the analogous phenomenon described in [1].

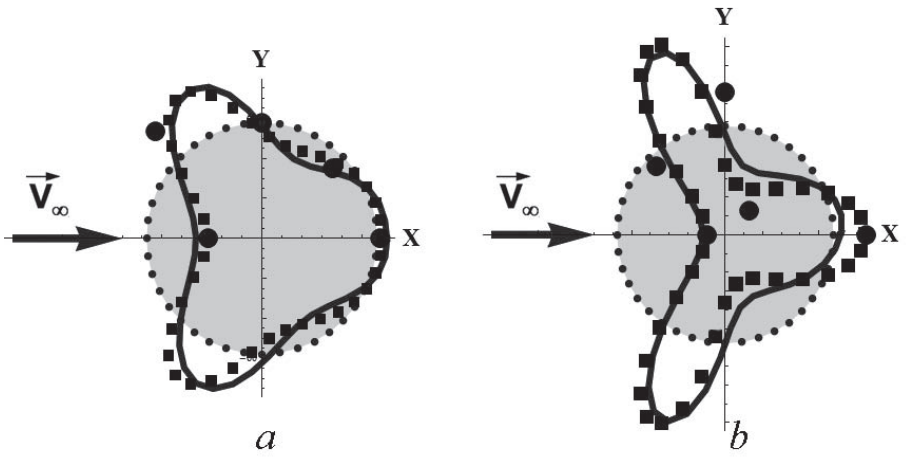

Figure 5: Displacement diagram for the middle ($z = 0$) cross-section for subcritical (a) and supercritical (b) flows. Dots ($\cdot$) correspond to initial cross-section; squares (■) denote results of FEM static analysis; circles (•) correspond to experimental data [12]; line (—) denotes the averaged shell displacement in numerical simulation (all displacements are enlarged by 1000 times)

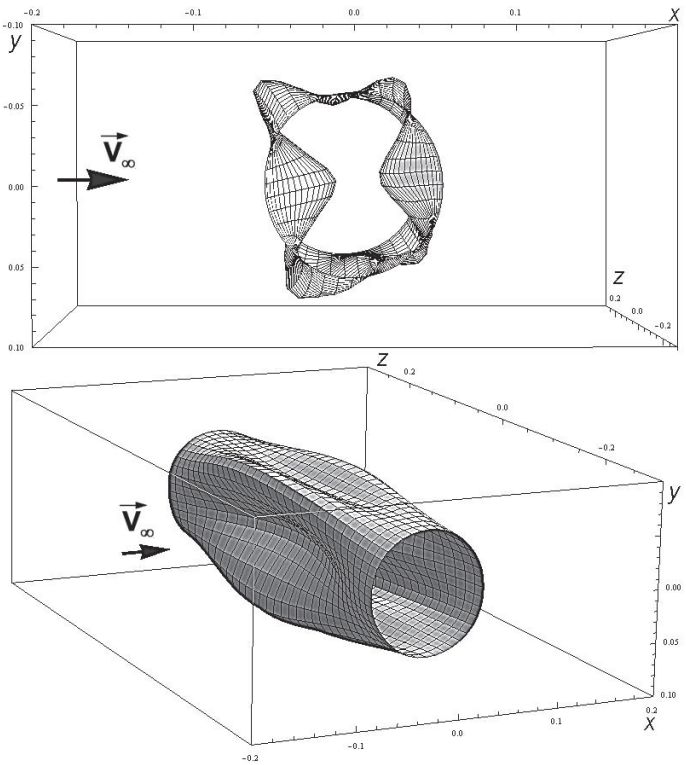

Figure 6: 3D deformed shape of the elastic shell (all displacements are enlarged by 1000 times)

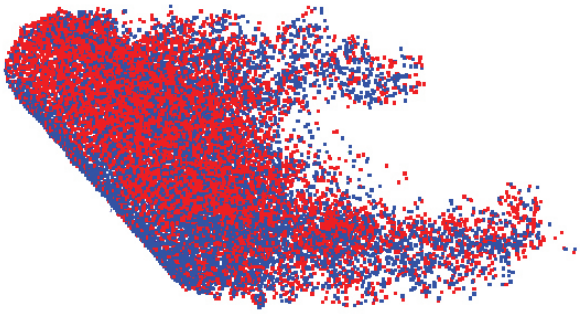

Figure 7: Vortex wake around the cylinder (colored points denote vortex fragmentons markers)

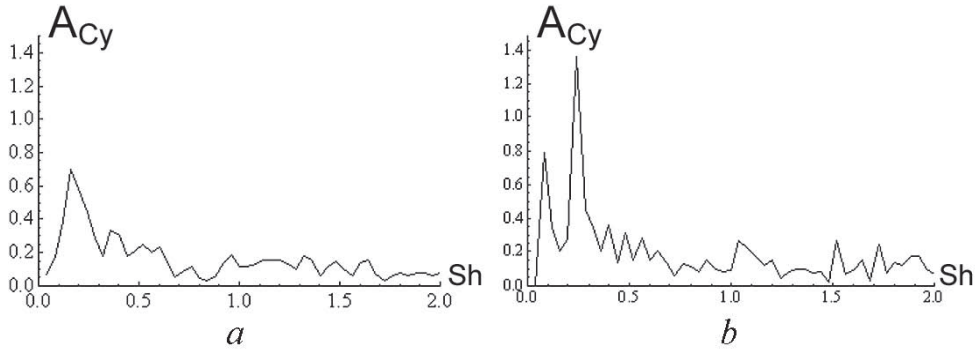

Figure 8: Lift coefficient spectrum for rigid (a) and elastic (b) cylinder

5 CONCLUSION

The numerical algorithm for complex coupled FSI-problem solving is developed and successfully verified. It is based on the combined usage of normal modes analysis method for shell dynamics simulation and vortex element method for flow simulation. The developed algorithm and original software allow to simulate directly vortex induced vibrations in the 3D flow for shells and structures with arbitrary shape.

ACKNOWLEDGEMENTS

The work was partially supported by Russian Federation President Grant for young scientists [proj. MK-3705.2014.08] and MSC Software Competence Center for Russian Aerospace industry in Bauman Moscow State Technical University.

REFERENCES

[1] Paidoussis, M.P., Price, S.J. and Suen, H.-C. Ovalling oscillations of cantilevered and clamped-clamped cylindrical shells in cross flow: An experimental study. *J. of Sound and Vibration* (1982) **83, 4**: 533–553.

[2] Belotserkovsky, S.M. and Lifanov,I.K. *Method of discrete vortices*. CRC Press (1994).

[3] Lighthill, M.J. Introduction. Boundary layer theory. In: Rosenhead, L. (ed.) *Laminar Boundary Layers*. Dover, Mineola (1963): 46–113.

[4] Cottet, G.-H., Koumoutsakos, P.D. *Vortex Methods: Theory and Practice*. CUP (2000).

[5] Ermakov, A.V. and Shcheglov, G.A. On applictaion of vortex element method for aeroelastic airfoil dynamics simulation. *ECCOMAS 2012, e-Book Full Papers* (2012): 6050–6063.

[6] Cottet, G.-H., Koumoutsakos, P.D. *Vortex Methods: Theory and Practice*. CUP (2000).

[7] Dowell, E.H. and Ilgamov, M. *Studies in Nonlinear Aeroelasticity*. Springer (2011).

[8] Marchevsky, I.K. and Shcheglov, G.A. 3D vortex structures dynamics simulation using vortex fragmentons. *ECCOMAS 2012, e-Book Full Papers* (2012): 5716–5735.

[9] Chorin, A.J. Numerical study of slightly viscous flow. *J. of Fluid Mechanics*. (1973) **57**: 785–796.

[10] Kempka, S.N., Glass, M.W., Peery, J.S. and Strickland, J.H. Accuracy considerations for implementing velocity boundary conditions in vorticity formulations. *SANDIA REPORT* (1996) **SAND96-0583, UC-700**.

[11] Dynnikova, G.Ya. An analog of the Bernoulli and Cauchy-Lagrange integrals for a time-dependent vortex flow of an ideal incompressible fluid. *Fluid Dynamics* (2000) **35, 1**: 24–32.

[12] Gafurov, M.B. and II'gamov, M.A. Deflection of a cylindrical shell of finite length upon transverse flow of a liquid around it. *Soviet Applied Mechanics* (1978) **14, 3**: 270–276.

[13] Parkinson, G.V. and Jandali, T. A wake source model for bluff body potential flow. *J. of Fluid Mech.* (1970) **40, 3**: 577–594.